Neuron, Vol. 16, 675–686, March, 1996, Copyright ©1996 by Cell Press

Knockout of Glutamate Transporters Reveals a Major Role for Astroglial Transport in Excitotoxicity and Clearance of Glutamate

Jeffrey D. Rothstein,* Margaret Dykes-Hoberg,* Carlos A. Pardo,† Lynn A. Bristol,* Lin Jin,* Ralph W. Kuncl,* Yoshikatsu Kanai,‡ Matthias A. Hediger,§ Yanfeng Wang,‖ Jerry P. Schielke,# and Devin F. Welty‖

*Department of Neurology
†Department of Neuropathology
Johns Hopkins University
Baltimore, Maryland 21287
‡Department of Pharmacology
Kyorin University School of Medicine
6-20-2 Shinkawa Mitaka
Tokyo, 181
Japan
§Department of Medicine
Renal Division
Brigham and Woman's Hospital
Harvard Medical School
Boston, Massachusetts 02115
‖Department of Pharmacokinetics and Drug Metabolism
#Department of Neuroscience Pharmacology
Parke–Davis Pharmaceutical Research
Ann Arbor, Michigan 48105

Summary

Three glutamate transporters have been identified in rat, including astroglial transporters GLAST and GLT-1 and a neuronal transporter EAAC1. Here we demonstrate that inhibition of the synthesis of each glutamate transporter subtype using chronic antisense oligonucleotide administration, in vitro and in vivo, selectively and specifically reduced the protein expression and function of glutamate transporters. The loss of glial glutamate transporters GLAST or GLT-1 produced elevated extracellular glutamate levels, neurodegeneration characteristic of excitotoxicity, and a progressive paralysis. The loss of the neuronal glutamate transporter EAAC1 did not elevate extracellular glutamate in the striatum but did produce mild neurotoxicity and resulted in epilepsy. These studies suggest that glial glutamate transporters provide the majority of functional glutamate transport and are essential for maintaining low extracellular glutamate and for preventing chronic glutamate neurotoxicity.

Introduction

Glutamate transport is the primary mechanism for the inactivation of synaptically released glutamate. Previous cell culture and cell fractionation studies have suggested that both astroglia and neurons are capable of high affinity glutamate transport. Subsequently, three glutamate transporters were cloned—EAAC1 (Kanai and Hediger, 1992), GLT-1 (Pines et al., 1992), and GLAST (Storck et al., 1992) in rat and rabbit—and the homologous transporters have been identified in human brain (Arriza et al., 1994). The localization of these transporters has revealed that EAAC1 is selectively localized to neurons (Rothstein et al., 1994, 1995), whereas GLT-1 (Rothstein et al., 1994, 1995; Lehre et al., 1995) and GLAST (Rothstein et al., 1994, 1995; Lehre et al., 1995) are astroglial transporters. The relative contribution of each of these transporters to the synaptic clearance of glutamate is not known. It has been suggested that under certain pathophysiological circumstances, such as acute cerebral ischemia and epilepsy, glutamate neurotoxicity is propagated due to failure or reversal of glutamate transport (Nicholls and Attwell, 1990; Rothstein et al., 1992; Attwell et al., 1993; Kanai and Hediger, 1995; Kanai et al., 1995b). Furthermore, a substantial loss of the glial glutamate transporter, GLT-1, has been demonstrated in the chronic degenerative disorder, amyotrophic lateral sclerosis (ALS; Rothstein et al., 1995). However, the exact role of glutamate transporter subtypes (e.g., neuronal versus glial) in neurotoxicity is not known. Selective inhibitors of glutamate transporter subtypes do not yet exist, so we employed antisense oligonucleotides to chronically inhibit the synthesis of individual glutamate transporter subtypes. From these experiments, we have gathered biochemical and morphological data that suggest that in the spinal cord, striatum, and hippocampus astroglial transporters GLT-1 and GLAST, but not the neuronal transporter EAAC1, are responsible for chronic glutamate-mediated neurotoxicity.

Results

Organotypic Spinal Cord Cultures

In the first set of studies, antisense oligonucleotides to GLT-1, GLAST, or EAAC1 were individually added to spinal cord organotypic cultures (Rothstein et al., 1993). These cultures were used because they have the advantage of maintaining the normal synaptic morphology, including astroglial/neuronal interactions, and have a stable population of motor neurons that can be studied for over two months (Rothstein et al., 1993). In addition, they afforded a relatively rapid, inexpensive method to screen various antisense sequences. Culture medium, including oligonucleotides and added drugs, was changed twice weekly. All experiments were performed with phosphorothioate oligonucleotides. One week after preparation of cultures, sense or antisense oligonucleotides (5 μM) were added to cultures. Antisense oligonucleotides to GLAST and GLT-1 decreased levels of GLAST by 88% $\pm$ 2% (SEM; n = 5) and GLT-1 by 67% $\pm$ 4% (n = 4) after 4 weeks of treatment (Figures 1A and 1B). Sense oligonucleotide did not affect tissue levels of the proteins (GLAST, 92% $\pm$ 2.3% [n = 8]; GLT-1, 103% $\pm$ 14% [n = 4], EAAC1 120% $\pm$ 15% [n = 4]) when compared to untreated control cultures. The effect of antisense treatment was transporter subtype specific; for example, antisense oligonucleotide to GLT-1 had no effect on the protein levels of GLAST (95%) or EAAC1 (93%). The neurotoxic effect of the loss

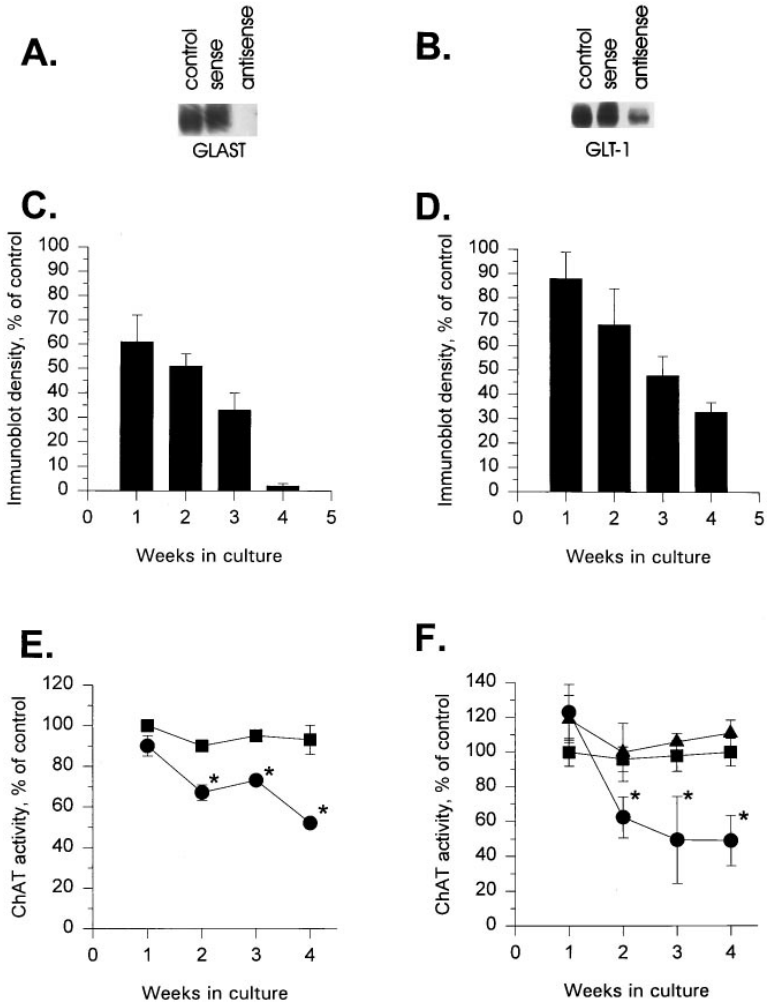

Figure 1. In Vitro Effect of Antisense Oligonucleotides to the Glutamate Transporters GLT-1 and GLAST on Protein Expression and Neuronal Survival

Antisense or sense oligonucleotides (5 μM) to GLAST or GLT-1 were chronically added to spinal cord organotypic cultures. At weekly intervals, cultures were harvested and homogenates were analyzed for GLAST or GLT-1 protein expression by immunoblot analysis (A and B) followed by semiquantitative densitometric evaluation (C and D). Lanes were loaded with exactly equal amounts of protein (15 μg). Choline acetyltransferase (ChAT) activity, an enzymatic marker of motor neurons, was measured in some homogenates at weekly time points following sense (squares) or antisense (circles) oligonucleotide treatment (E and F). GYKI-52466, a non-NMDA glutamate receptor antagonist, was added to cultures (100 μM) along with GLT-1 antisense oligonucleotide (F, triangles) to determine whether antisense-mediated motor neuron toxicity was due to glutamate. All time points in the figure represent the mean ± SEM of 2–7 determinations. Asterisks, $p < .05$ (compared with sense treatment by Student's t test). There was no statistically significant difference between sense-treated cultures and untreated control cultures.

of glutamate transporter was evaluated by measuring choline acetyltransferase (ChAT) activity in culture homogenates. In this preparation, ChAT is selectively localized to ventral motor neurons and can be used as a reliable marker for motor neuron viability. The loss of either GLAST or GLT-1 protein was toxic to motor neurons, as reflected by a progressive decline in spinal cord ChAT activity (Figure 1E), similar to previous studies using pharmacologic inhibition of glutamate transporters (Rothstein et al., 1993). Although antisense to EAAC1 produced a 75% ± 11% (SEM; n = 4) loss of protein, there was no associated motor neuron toxicity (data not shown). In organotypic cultures, degeneration of motor neurons following pharmacological inhibition of glutamate transport can be selectively antagonized by non-NMDA glutamate receptor antagonists (Rothstein et al., 1993; Rothstein and Kuncl, 1995). Similarly, the neurotoxicity associated with antisense oligonucleotide to GLT-1 was completely prevented by the non-NMDA antagonist GYKI-52466 (Figure 1F), thus confirming the specificity of the antisense effect.

Chronic Intraventricular Antisense Administration

To investigate more fully the role of each transporter subtype in the clearance of extracellular glutamate and in excitotoxicity, glutamate transporter subtype antisense oligonucleotides were chronically administered intraventricularly, via miniosmotic pumps. Rats were continuously treated for 7–10 days with intraventricular antisense oligonucleotide to either GLAST, GLT-1, or EAAC1. All sequences corresponded to untranslated and translated amino terminal regions of GLAST, GLT-1, or EAAC1 messenger RNA. Antisense, sense, or random oligonucleotides were administered at a dose of 10 nmol/day. Animals were observed daily during administration of the oligonucleotides. After 7–8 days, animals were sacrificed and brains were rapidly frozen. In some cases, animals were perfused at sacrifice for detailed histological evaluation of brain tissue.

Administration of either GLT-1 or GLAST antisense oligonucleotide produced a progressive motor syndrome (Table 1); within 3 days animals began to exhibit slowing of hindlimb movements, which progressed to include unstable gait, mildly paretic hindlimbs, and dystonic postures. By 7 days of treatment with antisense oligonucleotide to GLAST or GLT-1, most of the animals were no longer able to ambulate because of paretic hindlimbs. They continued to groom, eat, and appeared alert, although weights were reduced by ~28% ± 1.1% compared with sense or random oligonucleotide–

Table 1. Behavioral Effects of Intraventricular Administration of Antisense Oligonucleotides to Glutamate Transporter Subtypes

Antisense Treatment	Behavior	
	Motor Syndrome	Seizures
GLAST	17/17	1/17
GLT-1	10/10	1/10
EAAC1	7/14	12/14

Data presented as number of animals with specific behavior per number treated. Motor syndrome refers to a progressive motor impairment that typically begins with slowed hindlimb movements, ataxic unstable gait, culminating in hindlimb paresis.

treated animals. By contrast, administration of antisense oligonucleotides to EAAC1 reliably produced epilepsy, characterized initially by facial twitches and freezing behavior that began after 3–5 days of treatment. By 7 days, tonic forepaw extension and clonic seizures occurred (Table 1). Antisense oligonucleotide to EAAC1 also produced a motor syndrome in about one half of the treated animals. However, motor impairment tended to be less severe compared with that obtained with GLAST antisense oligonucleotide. Sense or random oligonucleotide for all three transporter subtype sequences were without any behavioral effect up to 10 days of treatment ($n = 6–10$ per group).

After 7 days of intraventricular administration, antisense oligonucleotide to GLAST produced an 84% $\pm$ 3.0% ($n = 12$) loss of striatal GLAST protein by quantitative immunoblots (Figures 2A–2C). This was associated with a 35% $\pm$ 4.0% ($n = 7$) loss of functional glutamate transport (Figure 2D). Immunohistochemistry confirmed that antisense oligonucleotides to GLAST diminished astroglial protein expression, whereas sense oligonucleotides had no effect (Figure 2B). There are a number of other important controls used to verify the specificity of the antisense effects: first, treatment with antisense oligonucleotides to GLAST did not affect striatal GLT-1 (95% $\pm$ 12% SEM of untreated control, $n = 4$) or EAAC1 protein (93% $\pm$ 15% SEM of untreated control, $n = 4$); second, missense oligonucleotides, containing the same proportion of each nucleotide subtype of the antisense sequence were not neurotoxic and had no effect on GLAST protein levels ($n = 2$); and, third, the administration of a mixture of GLAST sense and antisense oligonucleotides ($n = 2$) did not alter glutamate transport in striatal homogenates, had no effect on glutamate transporters subtypes when examined by immunoblots, and had no behavioral effect.

Similarly, 7 days of antisense oligonucleotides to GLT-1 ($n = 9$) produced a 58% $\pm$ 4.0% loss of striatal GLT-1 protein by immunoblot analysis (Figure 2C), but did not affect the protein levels of GLAST (92% $\pm$ 12% of untreated control, $n = 4$) or EAAC1 (109% $\pm$ 10% of untreated control, $n = 10$). The loss of GLT-1 protein produced a 56% $\pm$ 4.8% loss of functional glutamate transport in striatal homogenates ($n = 9$; Figure 2D). Finally, antisense oligonucleotides to EAAC1 delivered over 7 days intraventricularly ($n = 7$), decreased striatal EAAC1 protein by 78% $\pm$ 5.0% (Figure 2C) and produced a 22% $\pm$ 3% loss of glutamate transport in striatal homogenates ($n = 5$). The effect of antisense oligonucleotides to EAAC1 was specific, as immunoblots showed no alteration of either GLT-1 (96% of untreated control, $n = 2$) or GLAST (94% of untreated control, $n = 2$) proteins. Thus, the biochemical and behavioral effects of antisense oligonucleotides to glutamate transporter subtypes appeared to be specific for the individual antisense sequences.

The effect of antisense oligonucleotides on transporter mRNA was evaluated by ribonuclease protection assay. Seven days of GLAST antisense oligonucleotides did not alter tissue GLAST mRNA (0.056 $\pm$ 0.09; all mRNA data are expressed as mean $\pm$ SEM, arbitrary units representing the ratio of transporter mRNA to β-actin mRNA by volumetric analysis; $n = 2–9$ observations for each analysis) compared with control (0.053 $\pm$ 0.010). Similarly there was no effect of GLT-1 antisense oligonucleotides on GLT-1 mRNA (GLT-1 antisense = 0.25 $\pm$ 0.04; control = 0.24 $\pm$ 0.05) or EAAC1 antisense oligonucleotides on EAAC1 mRNA (EAAC1 antisense = 0.032 $\pm$ 0.004; control = 0.036 $\pm$ 0.006). The lack of effect of the antisense oligonucleotides on mRNA levels suggests that their biochemical actions are posttranscriptional.

Hippocampal glutamate transport and transporter proteins were also affected by intraventricular administration of antisense oligonucleotides. As shown in Figure 2E, individual antisense oligonucleotides inhibited the synthesis of their respective transporter proteins, and the magnitude of this effect was similar to that measured in the striatum. However, the contribution of each transporter to total tissue glutamate transport was different in the striatum (Figure 2F), with a smaller role for GLAST (19%) and greater role for EAAC1 (43%). However, similar to the striatum, astroglial glutamate transporters were responsible for the greatest proportion ($\sim$60%) of hippocampal glutamate transport. The intraventricular administration of antisense oligonucleotides did not alter transporter proteins or glutamate transport in more distant structures including spinal cord and cerebellum (data not shown).

As an additional control for the increased formation of intracellular RNA–oligonucleotide duplexes that could occur in astrocytes following the administration of GLT-1 or GLAST antisense oligonucleotides, some animals were treated with antisense to glial fibrillary acidic protein (GFAP), an astroglial specific protein. Antisense oligonucleotide to GFAP (5′-CAGAGGCGAGGTAGAA CG-3′), which decreased GFAP protein by 50% ($n = 2$), had no behavioral effect, and did not affect glutamate transport (95% untreated control) or glutamate transport proteins (GLAST, 98%; GLT-1, 93%; and EAAC1, 102% of untreated control). Antisense to GFAP was also used in organotypic spinal cord cultures for up to 4 weeks at a concentration of 5 μM ($n = 4$), and had no effect on motor neuron survival.

Effects of Antisense Oligonucleotides on Extracellular Glutamate

Because glutamate transport is believed to maintain low extracellular glutamate concentrations, we were interested in determining if all, or selected transporter subtypes, were responsible for this activity. As before,

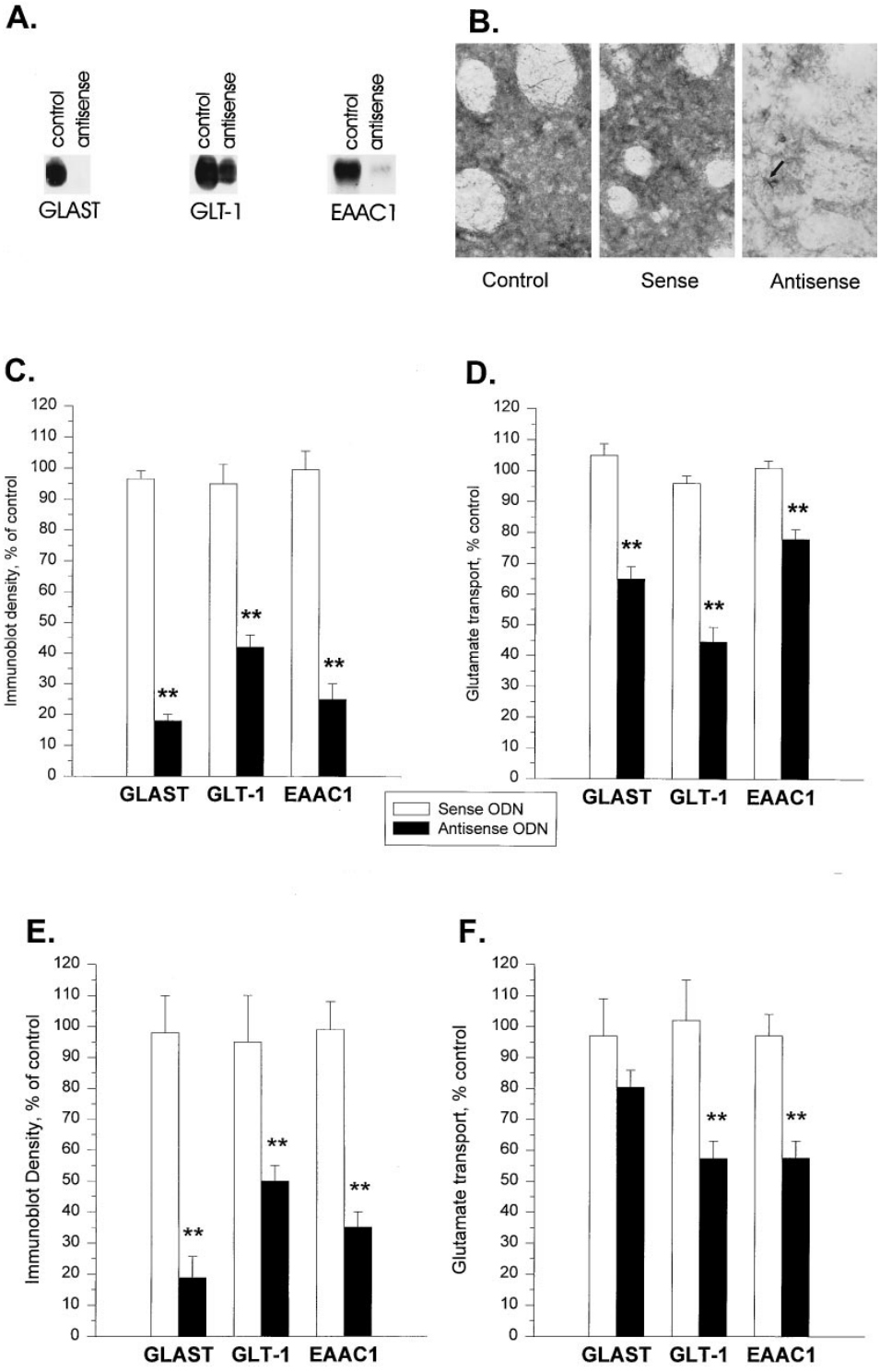

Figure 2. Analysis of Striatum and Hippocampus following In Vivo Administration of Oligonucleotides to Glutamate Transporter Subtypes GLAST, GLT-1, and EAAC1

Oligonucleotides were delivered intraventricularly over 7 days (10 nmol/day). (A) Striatal tissue was collected and immunoblotted for glutamate transporter subtypes (5) following treatment with antisense or sense oligonucleotide. For GLAST and EAAC1, each lane contains 15 μg protein homogenates, while each lane for GLT-1 immunoblot has 5 μg striatal protein. Random oligonucleotides had no effect on transporter protein levels (data not shown). (B) GLAST immunoreactivity in striatal tissue 7 days after chronic intraventricular infusions of GLAST sense or GLAST antisense oligonucleotides compared with untreated control striatum. Immunostaining was performed on tissue ipsilateral to intraventricular site. The reduction of neuropil GLAST immunoreactivity allows identification of individual GLAST-positive astrocytes (arrow). (C) Densitometric analysis of immunoblots performed on GLAST, GLT-1, and EAAC1 in striatal tissue following sense or antisense oligonucleotide administration. (D) Glutamate transport was measured in homogenates of striatal tissue following chronic treatment with an individual antisense or sense

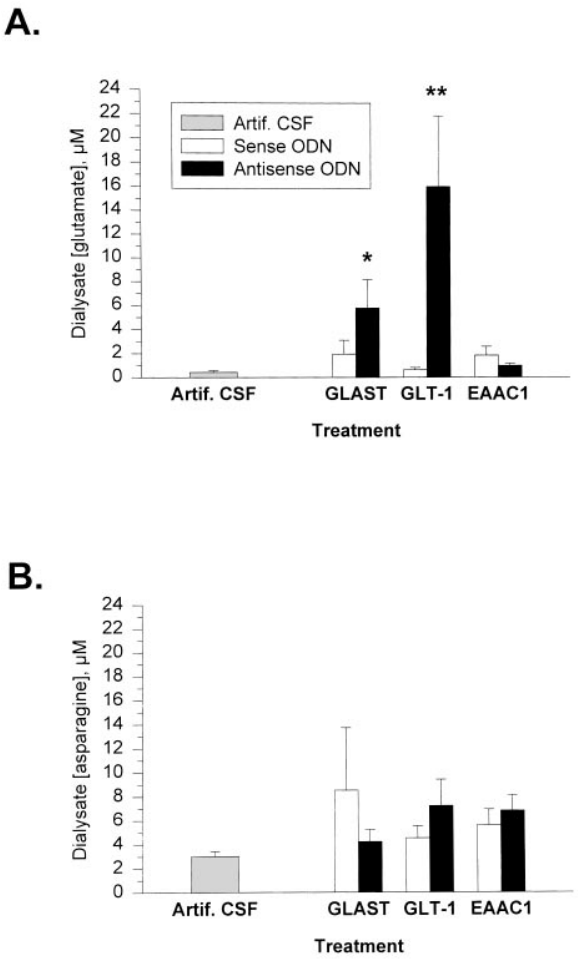

Figure 3. Microdialysis Determination of Extracellular Glutamate and Asparagine Concentration following 7 Days of Intraventricular Oligonucleotides to Glutamate Transporter Subtypes

Microdialysis probes were placed in the striatum ipsilateral to intraventricular infusion cannulas in animals treated with antisense or sense oligonucleotides to GLAST, GLT-1, or EAAC1. Dialysate was analyzed for both glutamate (A) and aspargine (B); 4–7 animals were studied for each oligonucleotide. Statistical significance of intraventricular antisense treatment compared to sense treatment: asterisk, $p < .05$; double asterisk, $p < .01$. ODN, oligonucleotide.

animals were treated with sense or antisense oligonucleotides to individual transporter subtypes by chronic intraventricular infusion. After 7 days of treatment, microdialysis probes were placed in the ipsilateral striatum to sample extracellular amino acids. The loss of either glial glutamate transporter, but not the neuronal transporter, was sufficient to produce a tonic rise in extracellular glutamate levels. Glutamate concentrations in the microdialysate were markedly elevated almost 32-fold ($p < .01$) after GLT-1 antisense oligonucleotide treatment, and about 13-fold ($p < .05$) after GLAST antisense treatment (Figure 3A). Antisense oligonucleotides to EAAC1 did not affect extracellular glutamate levels in striatum. The rise in extracellular glutamate associated with the loss of each transporter subtype (Figure 3A) correlated significantly ($p < .03$) with the estimated percent contribution of each transporter to total glutamate transport (see Figure 2D).

Because GLAST and GLT-1 antisense treatments produce striatal neurotoxicity (see below), these elevations could have reflected damage and release from neurons rather than the steady-state rise in extracellular glutamate due to the loss of transporter. To address that possibility, extracellular asparagine was also monitored during microdialysis. As shown in Figure 3B, there was no increase in asparagine concentrations after 7 days of GLAST antisense treatment. Thus, the changes in extracellular glutamate likely reflect the loss of the transporter protein.

Histological Evaluation of Antisense Oligonucleotides

To address more directly whether sustained inhibition of subtype specific transport can cause excitotoxic neuronal damage in the whole animal, we administered antisense oligonucleotides intraventricularly to either GLAST, GLT-1, or EAAC1 by miniosmotic pumps. After 7 days, animals were sacrificed, and striatal and hippocampal tissue was examined by light and electron microscopy for evidence of cellular degradation.

The loss of either GLAST or GLT-1 protein, following antisense treatment, produced neurotoxicity seen at both the light and electron microscopic level (see Figures 5 and 6). When examined under low magnification, there was no gross tissue necrosis (Figure 4) following antisense treatment (Figures 4D–4F) compared with several controls: untreated animals (Figure 4A), artificial cerebrospinal fluid (ACSF) control (Figure 4B), or sense oligonucleotide (GLT-1) control (Figure 4C). Ventricular enlargement was typically seen on the side of intraventricular cannulas (Figures 4B–4E), as well as occasional mild inflammation associated with cannula tracts (Figures 4C–4F).

Closer inspection of striatal neurons confirmed the overall preservation of neuronal populations in antisense-treated tissue compared with sense-treated and ACSF-treated tissue (Figures 5A–5C). However, striatal neurons in animals treated with antisense oligonucleotides appeared enlarged and distorted following GLT-1 antisense (Figure 5C) and GLAST antisense (not shown) treatment.

To evaluate more completely the nature of these morphological changes, semithin plastic sections and electron microscopy were performed. Semithin plastic sections revealed neurotoxic changes including frequent cytoplasmic vacuoles and occasional degenerating neurons (Figures 5D–5F). Neuronal cytotoxicity was most commonly seen following loss of either GLAST or

oligonucleotide as indicated. (E) Densitometric analysis of immunoblots performed on GLAST, GLT-1, and EAAC1 in hippocampus following sense or antisense oligonucleotide administration. Each bar represents the mean ± SEM of 5–12 determinations. (F) Glutamate transport was measured in homogenates of hippocampal tissue following chronic treatment with an individual antisense or sense oligonucleotide as indicated. Each bar represents the mean ± SEM of 5–12 for (C) and (D), and 4–6 determinations for (E) and (F). Statistical significance of intraventricular antisense treatment compared to sense treatment: double asterisks, $p < .01$. ODN, oligonucleotide.

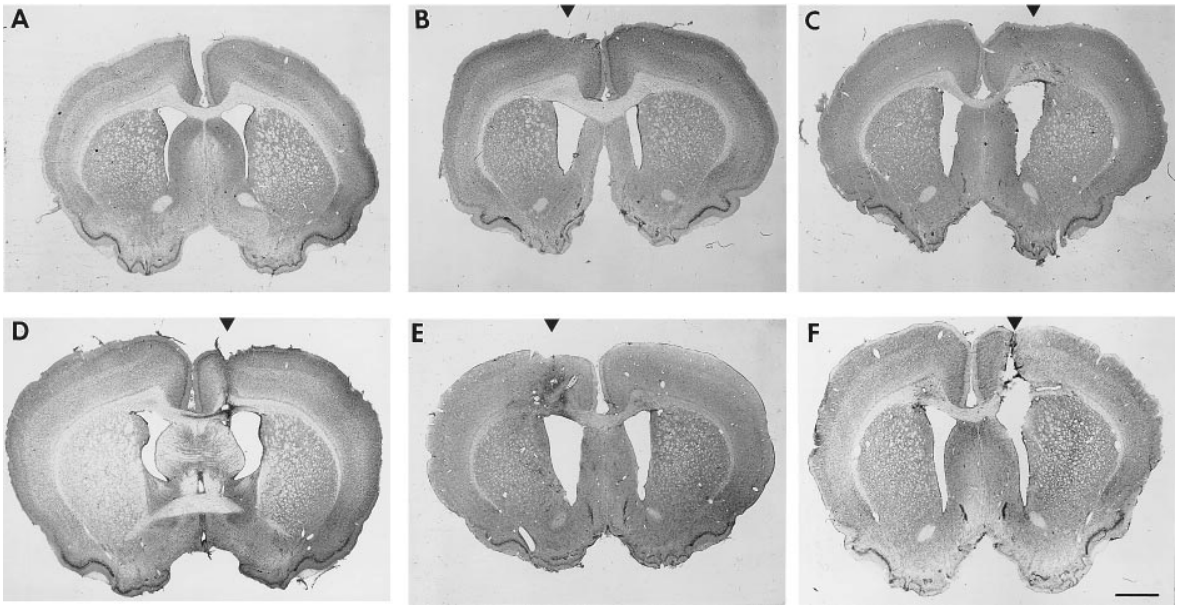

Figure 4. Coronal Sections of Rat Brain following Chronic Intraventricular Oligonucleotides

Animals were treated for 7 days with antisense oligonucleotides to GLAST (D), GLT-1 (E), or EAAC1 (F) compared to three different controls: untreated (A), ACSF-treated (B), or sense (GLT-1; C) oligonucleotide-treated animals. At this low magnification of cresyl violet–stained sections, there was gross tissue necrosis seen following these antisense treatments. Ventricular distortion was sometimes seen on the side of intraventricular cannulas (arrowheads), along with cannula tract inflammation. Scale bar, 1.15 mm.

GLT-1 proteins (Table 2; Figures 5D–5F). Other cellular elements appeared unaffected by GLAST or GLT-1 antisense treatment. Antisense EAAC1 treatment rarely produced cellular changes at the light microscopic level of observation in the striatum (Table 2), although occasional vacuolated neurons were observed (Figure 5D) in cortex along with vacuolization of hippocampal neuropil (Figure 5F). Sense treatment did not produce any evidence of significant cytotoxicity (see Figures 4–6).

Quantification of these changes in both striatum and hippocampus, by examination of semithin plastic sections (Table 2), confirmed the increase in cytotoxicity associated with antisense treatment for each of the glutamate transporters subtypes. The loss of GLAST or GLT-1 protein appeared to produce more cytotoxicity than the loss of EAAC1 when examined in either striatum or hippocampus. There was no significant cytotoxicity seen in either brain region following chronic sense or ACSF treatment.

Electron microscopic evaluation of striatal and hippocampal neurons 7 days after continuous intraventricular infusion of the antisense oligonucleotide to GLAST and GLT-1 corroborated the light microscopic observations, in that the most common cytological abnormalities in neurons consisted of the formation of multiple vacuoles of heterogenous size occupying the cytoplasmic compartment (Figures 6C–6E and 6I). The vacuoles appeared to be formed from dilated endoplasmic reticulum, mitochondria (Figure 6D, inset), and lysosomal vacuoles consisting of heterogenous material (Figure 6D). In some neurons, the Golgi apparatus appeared dilated. In other affected neurons, there was an abundance of early degenerative changes that consisted of multiple lamellated intracytoplasmic structures, some of them resembling lysosomes. Occasional neurons appeared to be undergoing a complete disintegration. In many areas within the striatum and hippocampus, there was widespread swelling of dendrites, which sometimes contained abnormal swollen mitochondria (Figures 6C, 6D, and 6H). These ultrastructural changes are similar to those observed in models of excitotoxicity (Olney, 1969; Olney et al., 1983; Hajos et al., 1986). Animals treated with EAAC1 antisense oligonucleotide had little ultrastructural changes in the striatum, although occasional enlarged dendrites contained vacuoles (Figure 6F). In the hippocampus, there was more extensive dendritic swelling associated with the loss of EAAC1 (Figure 6H). There was no evidence of cellular degeneration, by light microscopic or electron microscopic observation, with sense GLAST, GLT-1, or EAAC1 oligonucleotide administration.

Discussion

Together, these in vitro and in vivo studies demonstrate that the high affinity glutamate transporters GLAST and GLT-1 are important in maintaining low extracellular glutamate concentrations and that elimination of either protein produces a tonic increase in extracellular glutamate resulting in neuronal degeneration. By antisense methodologies, it appears that the bulk of glutamate clearance occurs through these astroglial transporters. Although they are not localized in the synaptic cleft (Rothstein et al., 1994, 1995; Lehre et al., 1995), their function to maintain low extracellular glutamate must be critical to preventing glutamate toxicity.

The administration of the antisense oligonulceotides

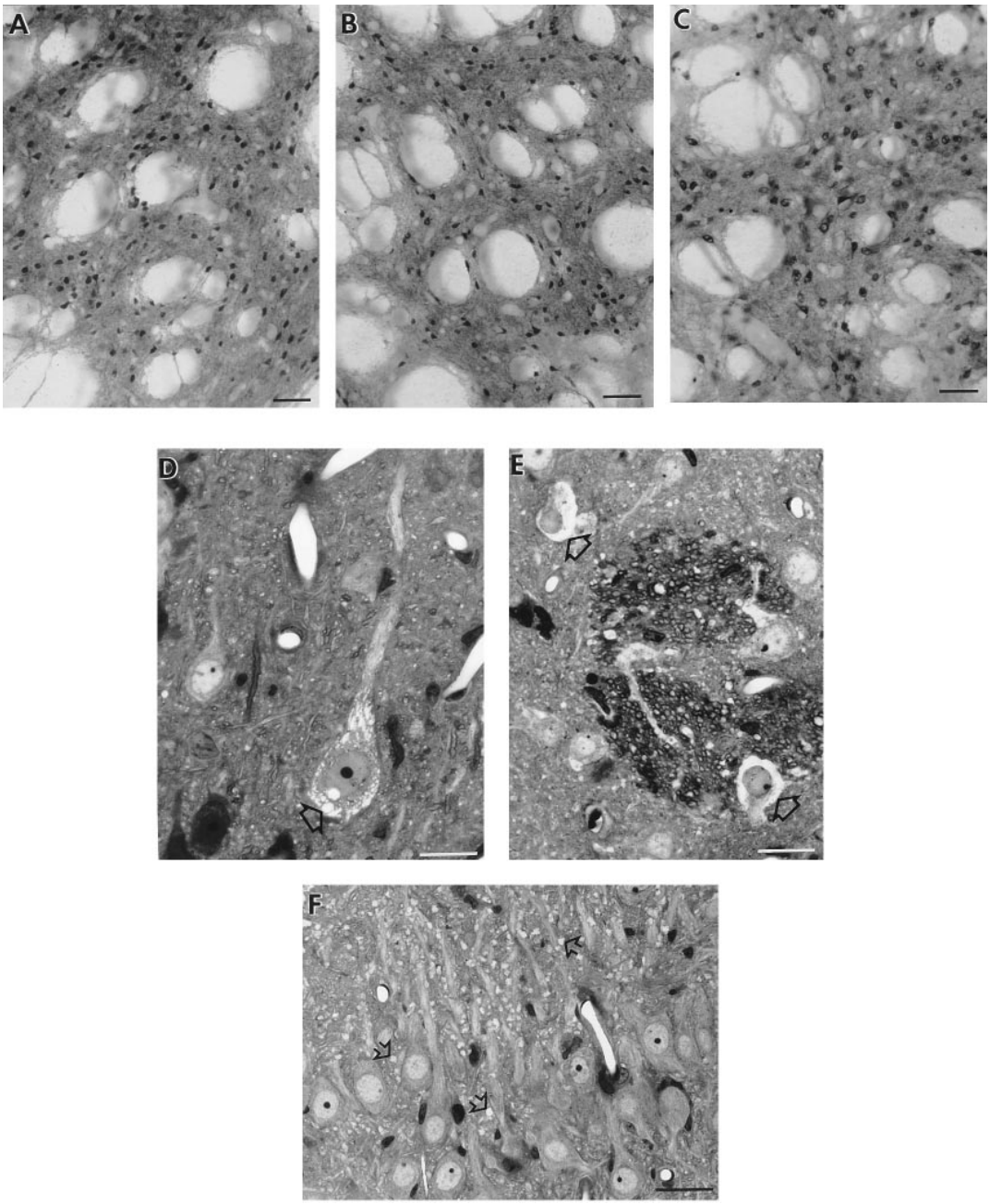

Figure 5. Intraventricular Administration of Antisense Oligonucleotides to Glutamate Transporter Subtypes Produced Cytotoxic Abnormalities in Surrounding Cortex, Striatum, and Hippocampus

Calbindin D-28 immunoreactivity in the striatum after three treatments: ACSF (A), GLT-1 sense oligonulceotide (B), GLT-1 antisense oligonucleotide (C). Neurons were grossly preserved in number following GLT-1 antisense treatment (C) compared to ACSF control (A) or GLT-1 sense-treated (B) animals. However, neurons appeared vacuolated and enlarged after GLT-1 antisense. Closer inspection of semithin plastic sections revealed antisense-induced cytotoxicity. (D) EAAC1 antisense treatment produced occasional neuronal cytotoxicity as reflected by numerous cytoplasmic vacuoles (arrow) in a cortical pyramidal neuron. (E) GLT-1 antisense oligonucleotides produced vacuolar degeneration of many striatal neurons (arrows). (F) EAAC1 antisense treatment produced extensive neuropil vacuolation in the hippocampus. Sections were stained with toluidine blue. Scale bar, 50 μm (A–C); 15 μm (D and E); 25 μm (F).

appeared to produce selective knockout of individual transporter subtypes. Random and sense oligonucleotide sequences had no effect on protein function or protein levels, thus confirming the selectivity of this method. In vitro neuroprotection with the non-NMDA antagonist GYKI-52466 also confirmed the specificity of this method.

Interestingly, the loss of either glial transporter produced a progressive motor deficit that may be a consequence of neuronal cytotoxicity and/or degeneration.

Table 2. Quantification of Abnormal Neurons following Administration of Antisense Oligonucleotides to Glutamate Transporter Subtypes

Region	Artificial CSF Control	GLAST		GLT-1		EAAC1	
		Antisense	Sense	Antisense	Sense	Antisense	Sense
Striatum	0	4.8 ± 0.44**	0	2.4 ± 0.23**	0	0.8 ± 0.23**	0
Hippocampus	0.1 ± 0.04	3.0 ± 0.25**	0	4.25 ± 0.44**	0.12 ± 0.04	1.1 ± 0.15**	0

After 7 days of intraventricular administration, antisense oligonucleotides to all three glutamate transporters produced significant neurotoxicity (e.g., vacuolization), while ACSF or sense oligonucleotides had no effect on neuronal morphology. Data are presented as the number of abnormal neurons per high power (1000×) microscopic field. Each value is the mean of 4–12 animals in which abnormal neurons were counted in 10 random high power fields from semithin plastic sections of striatum or hippocampus (dentate gyrus). Double asterisk, $p < .01$ compared to ACSF control.

Alternatively, the excessive extracellular glutamate, observed following the loss of the glial transporters, could produce persistent synaptic depolarization and disrupt neural circuitry.

Experiments on bulk isolated neurons and glia, and later, on cultured neurons and astrocytes, have demonstrated that these cellular populations are capable of high affinity glutamate transport (Hertz, 1979). However, the relative contribution of each population is unknown, and could only be inferred from analysis of transporter kinetics (Hertz, 1979). There are no specific inhibitors of neuronal versus glial glutamate transport, nor are there specific inhibitors that can distinguish molecular subtypes. Although localization studies suggest differential distributions of the transporter proteins, immunocytochemical techniques are not adequate to assess the functional contribution of transporter subtypes. By employing antisense oligonucleotides, the contribution of each transporter subtype to total clearance of extracellular glutamate can now be inferred. These studies suggest that the contribution of each glutamate transporter subtype to glutamate transport varies by brain region. The glial glutamate transporters, GLT-1 and GLAST, provide the major contribution to high affinity glutamate transport—approximately 80% in the striatum and 60% in the hippocampus (see Figure 2D)—whereas EAAC1 appears to account for about 20% of striatal and 40% of hippocampal glutamate transport. Thus, the three known glutamate transporters account for almost all functional glutamate transport in the striatum and hippocampus. Additional support for this conclusion comes from the microdialysis studies that demonstrated that both the glial transporters, but not the neuronal transporter, account for maintenance of low extracellular glutamate levels. A fourth novel glutamate transporter has been identified in humans, but it appears to be restricted to the cerebellum (Fairman et al., 1995). Since these experiments were focused on the three high affinity glutamate transporters known to be present in the striatum, they cannot rule out the contribution, albeit small, of other uncloned glutamate transporters.

Glutamate transport has been postulated to be critical in the maintenance of low extracellular glutamate to protect against excitotoxic cell damage. Nonselective transport blockers, used in vitro, have been shown to raise extracellular glutamate, to alter postsynaptic potentials (Isaacson and Nicoll, 1993; Sarantis et al., 1993; Mennerick and Zorumski, 1994), and to result in neurotoxicity (Robinson et al., 1993; Rothstein et al., 1993; Barks and Silverstein, 1994). However, some studies suggest that inhibition of glutamate transport would actually result in postsynaptic receptor desensitization and presynaptic inhibition of further glutamate release (Maki et al., 1994; Tong and Jahr, 1994), thus moderating neurotoxicity. Furthermore, the relative role of neuronal versus astroglial clearance of glutamate in excitotoxicity is not known. However, the antisense inhibition of individual transporter subtypes now provides histological evidence that the loss of either astroglial glutamate transporter is sufficient to cause excitoxicity, as reflected by the vacuolar degeneration of neurons.

Surprisingly, EAAC1 antisense oligonucleotide treatment caused neither drastic neurodegeneration nor extracellular glutamate elevation in the striatum. This may be because, under normal conditions, neuronal glutamate transporters operate at or near equilibrium (Kanai and Hediger, 1995; Kanai et al., 1995b). In neurons, intracellular glutamate concentration is thought to be around 10 mM, whereas glutamate concentration in astroglia is considerably lower (50 to several hundred micromolar). The lower glutamate concentration in glial cells may be due to the rapid conversion of glutamate to glutamine, by glutamine synthetase that is present selectively in astroglia (Riepe and Norenberg, 1977; Norenberg and Martinez-Hernandez, 1979; Attwell et al., 1993; Pow and Robinson, 1994). Therefore, neurons may not have a great capacity to take up extracellular glutamate, whereas astroglia have a huge capacity to remove extracellular glutamate. This hypothesis is supported by the observation that EAAC1 contributes ~20%–40% of glutamate transport.

The fact that neuronal glutamate transporters are almost at equilibrium suggests that the neuronal transporters could run in the reverse direction more easily. Reversal of glutamate transport has been proposed as a mechanism of excitotoxicity under conditions of energy failure, as in cerebral ischemia (Nicholls and Attwell, 1990; Attwell et al., 1993; Kanai and Hediger, 1995; Kanai et al., 1995b). Our experiments do not rule out the possibility that EAAC1 could contribute to excitotoxicity as a consequence of transport reversal. Loss of EAAC1 protein was sufficient to produce some behavioral abnormalities, suggesting that disturbances of intrasynaptic glutamate by the loss of neuronal glutamate transport could alter some synaptic events, perhaps by persistent depolarization or alteration in presynaptic transmitter release. In addition, EAAC1 protein has been localized to inhibitory GABAergic neurons, such as the cerebellar Purkinje cell (Rothstein et al., 1994). Since glutamate is a precursor for GABA synthesis, EAAC1-mediated

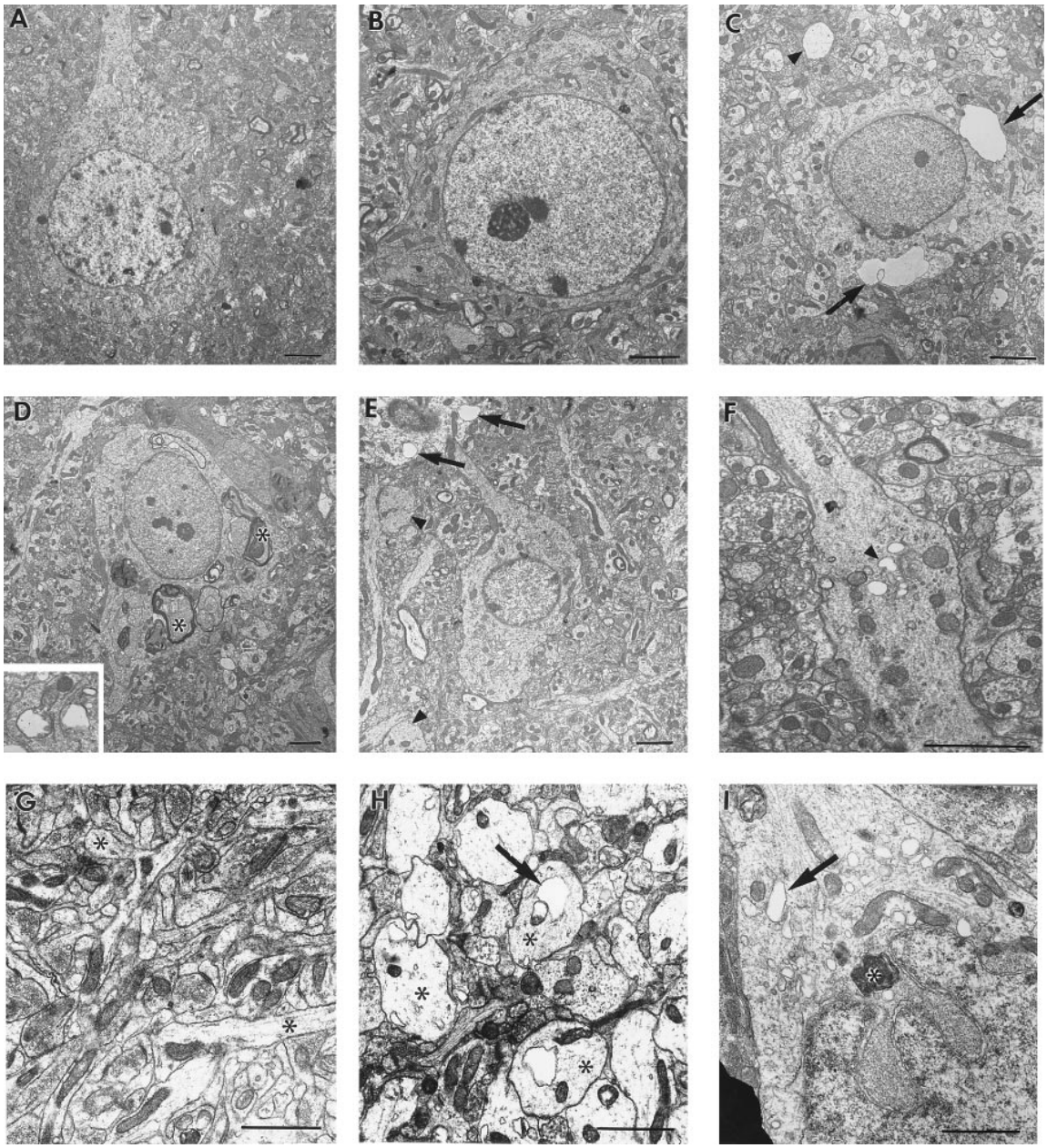

Figure 6. Qualitative Evaluation of Striatal and Hippocampal Neurotoxicity following Chronic Intraventricular Administration of Antisense Oligonucleotides to GLAST, GLT-1, or EAAC1

(A) Control striatum from an animal receiving intraventricular ACSF demonstrating normal-appearing neurons and neuropil. (B) Chronic administration of sense oligonucleotide to GLAST had no effect on striatal neurons or neuropil. Similarly, there was no effect of GLT-1 or EAAC1 sense oligonucleotides (data not shown). Antisense oligonucleotides to GLAST produced marked pathological changes in striatal neurons (C and D) including cytoplasmic vacuolization (arrow), massive dendritic dilatation (arrowhead), large intracytoplasmic multilamellated structures (asterisks) and occasional dilated mitochondria (inset). (E) Antisense oligonucleotides to GLT-1 produced cytoarchitectural changes identical to GLAST: cytoplasmic vacuolization (arrows) and dendritic swelling (arrowheads). (F) EAAC1 antisense oligonucleotide produced little striatal pathology. Rarely, dendritic vacuoles were observed (arrowheads). (G) Control hippocampal neuropil of an animal following intraventricular ACSF demonstrating normal-appearing synapses and dendrites (asterisks). Similarly, there was no effect of EAAC1, GLAST, or GLT-1 sense oligonucleotides (data not shown). (H) Chronic treatment with EAAC1 antisense oligonucleotides resulted in marked dilatation of dendrites (asterisks) and mitochondria (arrow), which contrasted with its mild cytotoxic effects in the striatum. Rarely, neurons with dilated mitochondria and endoplasmic reticulum were seen following EAAC1 antisense oligonucleotide treatment (data not shown). (I) Antisense oligonucleotides to GLAST produced pathological changes in hippocampal neurons similar to that seen in the striatum: lysosomes (asterisk), vacuoles (arrow), and dilated endoplasmic reticulum. Scale bar, 2 μm (A–F); 1 μm (G–I).

glutamate transport could also have a functional role in GABA metabolism and neurotransmission.

Abnormal function of glutamate transporters has been implicated in acute and chronic neurological insults. A loss of glutamate transport in brain membranes has been found in the neurodegenerative disorder amyotrophic lateral sclerosis (Rothstein et al., 1992, 1995; Shaw et al., 1994), and more recent studies indicate that the defect is specific for the GLT-1 protein (Rothstein et al., 1995). The antisense oligonucleotide experiments suggest that the loss of either glial glutamate transporter could account for, or contribute to, neuronal degeneration in that disorder. The behavioral syndrome associated with EAAC1, seizures and paresis, also suggests that dysfunction of this neuronal transporter could be important in other neurological disorders such as epilepsy.

Experimental Procedures

Organotypic Cultures

Organotypic spinal cord cultures were prepared from 8-day-old rat pup lumbar spinal cords, as described previously (Rothstein et al., 1993). Culture media (50% MEM–HEPES [25 mM], 25% heat-inactivated horse serum, and 25% Hanks' balanced salt solution [GIBCO] supplemented with D-glucose [25.6 mg/ml] and glutamine [2 mM], at a final pH of 7.2) was changed twice weekly. ChAT activity was measured as described previously (Rothstein et al., 1993). Phosphorothioate oligonucleotides were added with each biweekly culture media change for a final concentration of 5 μM. Other concentrations (up to 20 μM) were examined, and optimum results were obtained with 5 μM. All oligonucleotides were reconstituted with culture medium, then filtered before addition to cultures (0.2 μm). Cultures were treated with oligonucleotides for up to four weeks in culture. At weekly intervals, tissue was collected and homogenized. Aliquots of tissue homogenates were analyzed for ChAT activity or immunoblotted for glutamate transporter subtypes (Rothstein et al., 1994, 1995).

Intraventricular Antisense Administration

Male Sprague–Dawley rats (250 g) were implanted with stainless steel cannulas (stereo coordinates: −0.8 mm anterior–posterior; −1.5 mm lateral; approximately −4.8 mm dorsoventral) in the right lateral ventricle. Correct placement of cannulas was confirmed in animals at the time of sacrifice. Phosphorothioate oligonucleotides were infused intraventricularly (1 μl/hr) using mini-osmotic pumps (Alzet #2002, Alza Corp., Palo Alto, CA). Lyophilized oligonucleotides were reconstituted in ACSF (0.14 mM NaCl, 3 mM K^+, 1.25 mM Ca^{2+}, 0.48 mM HPO_4, 21 mM HCO_3, 3.4 mM glucose, 2.2 mM urea, pH 7.4 [Merlis, 1940]) at a concentration of 2.5 mg/ml. Freshly reconstituted oligonucleotides were dialyzed [SpectraPor cellulose ester, MW cutoff 2000 (Thomas Scientific)] overnight in 2 l ACSF (4°C), then filtered (0.22 μm) prior to use. Oligonucleotides were loaded into mini-osmotic pumps, then connected to intraventricular cannulas by polyethylene tubing, and placed subcutaneously. In some experiments, rats (n = 2) were treated intraventricularly with a mixture of sense and antisense oligonucleotides for 7 days. Prior to administration, oligonucleotides (500 ng GLAST sense oligonucleotide and 100 ng antisense oligonucleotide dissolved in ACSF) were dialyzed, filtered, then mixed overnight at room temperature.

Antisense Oligonucleotides

Initial studies indicated that consistent inhibition of glutamate transport was obtained with phosphorothioate derivatives. Phosphodiester oligonucleotides were used owing to the rapid degradation of unmodified oligonucleotides (Whitesell et al., 1993; Wagner, 1994). In all cases, the sequences chosen were novel and unrelated to any other nucleotide sequence in GenBank. Sequences for the sense and antisense oligonucleotides of GLAST, GLT-1, and EAAC1 were identical in all experimental paradigms used. Controls for the effects of antisense oligonucleotides included sense strands and "random" oligonucleotides in which the proportions of each adenine, thymidine, guanine, and cytosine nucleotide were identical to that of the antisense strand, but the sequence was randomly assigned. Sequences for the oligonucleotides used were as follows: sense GLAST, 5′-GAAAGATAAAATATGACAAAAAGCAAC-3′ (corresponding to nucleotides −12 to 15); antisense GLAST, 5′-GTTGCTTTTTGT CATATTTTATCTTTC-3′; sense GLT-1, 5′-ATCAACCGAGGGTGCCA ACAATAT-3′ (corresponding to nucleotides 6 to 29); antisense GLT-1, 5′-ATATTGTTGGCACCCTCGGTTGAT-3′; sense EAAC1, 5′-GCTCGGGATGCGACTGGC-3′ (corresponding to nucleotides 17 to 34); antisense EAAC1, 5′-GCCAGTCGCATCCCGAGC-3′. Additional random oligonucleotide sequences for the intraventricular experiments included: GLAST, 5′-TGTCGTTTTGTTATCTATATTCTTT CT-3′; GLT-1, 5′-AATTGTGTTAGCCCCCTCTGTTGA-3′; EAAC1, 5′-GCGGATCCGTACGCCCAG-3′. Several other antisense sequences for GLAST, EAAC1, and GLT-1 were investigated in preliminary in vitro studies. Sequences were based on the rat GLT-1 (Pines et al., 1992), rat GLAST (Storck et al., 1992), and rat EAAC1 (Kanai et al., 1995a). These oligonucleotides, which had lengths ranging from 18- to 27-mer, had a variety of different start sites relative to the gene's initiator codon. The efficacy of these antisense sequences at inhibiting the synthesis of transport protein varied, some with no effect on the protein (e.g., GLT-1 antisense, 5′-CTCGGTTGATGCCA TGGCGTGGGGAAC-3′).

Immunoblots

Animals were sacrificed by decapitation, and brains were rapidly removed and placed on a chilled aluminum block (4°C). Coronal sections of brain were sliced at 1–2 mm intervals from the cerebellum to the olfactory bulbs. The striatum and hippocampus were microdissected from these slices and homogenized in Krebs buffer (pH 7.4). Immunoblots of the striatal or hippocampal homogenates were prepared with affinity-purified polyclonal oligopeptide antibodies to GLAST, GLT-1, and EAAC1 as described previously (Rothstein et al., 1994, 1995). For both GLT-1 and EAAC1, carboxy-terminal antibodies were used. For GLAST, both a carboxy-terminal antibody (Rothstein et al., 1994) and another monospecific amino-terminal antibody (sequence: KSNGEEPRMGSRMGR) were employed. Both GLAST antisera produced identical immunoblots (J. Rothstein et al., unpublished data). In some experiments, identical aliquots of striatal tissue from animals treated with antisense oligonucleotides were analyzed simultaneously for all three transporters by immunoblots, and immunoblot density was quantified by laser densitometry (Molecular Dynamics, CA).

Immunohistochemistry

The brains of 250 g male Sprague–Dawley rats (n = 7) were prepared for immunocytochemical evaluation of GLT-1, GLAST, and EAAC1 as described previously (Rothstein et al., 1994). Rats were perfused intra-aortically with 4% paraformaldehyde in phosphate-buffered saline. Brains were removed, blocked, and postfixed (1 hr, 4°C), then cryoprotected (overnight, 4°C) in 20% glycerol, phosphate-buffered saline. Coronal sections (40 μm) were cut on a sliding microtome and were transferred to cold Tris-buffered saline (TBS; pH 7.2). For some experiments, coronal sections were dehydrated with ethanol and stained with cresyl violet. For immunohistochemical evaluation, sections were pre-incubated (1 hr) with 4% normal goat serum diluted in 0.1% Triton X-100 (TX)/TBS and were then incubated (48 hr, 4°C) in the affinity-purified transporter antibody, at a concentration of 0.2 μg/ml for GLAST, 0.06 μg/ml for EAAC1, and 0.17 μg/ml for GLT-1 of IgG per milliliter in 0.1% TX, 2% normal goat serum, TBS. For some experiments, tissue was stained with antibody to calbindin D-28 (Sigma Immunochemicals, St. Louis) at 1:2000. Following primary antibody incubation, sections were rinsed (30 min) in TBS, incubated (1 hr) with goat anti-rabbit (Cappel) diluted 1:200 in TBS with 2% normal goat serum and 0.1% TX. After rinsing in TBS, the sections were incubated (1 hr) in rabbit peroxidase–antiperoxidase complex (Sternberger Monoclonals, Baltimore, MD) diluted 1:300 in TBS with 2% normal goat serum. For calbindin D-28 staining, tissue was incubated with goat-anti-mouse 1:200, followed by incubation mouse peroxidase–antiperoxidase complex (Sternberger Monoclonals, Baltimore, MD) diluted 1:200. After the

final incubation, sections were rinsed (30 min) in TBS and developed using a standard diaminobenzidine reaction.

Electron Microscopy

The brains of 250 g male Sprague–Dawley rats were prepared for both light and electron microscopic evaluation as described previously (Rothstein et al., 1994). The striatum or hippocampus from at least 4 animals for each oligonucleotide treatment group was examined by electron microscopy. Rats were perfused intra-aortically with 4% paraformaldehyde/0.1% glutaraldehyde/15% saturated picric acid/2% acrolein or with 4% paraformaldehyde alone, both prepared in phosphate-buffered saline. Brains were removed, blocked, and postfixed (1 hr, 4°C). Brains for light microscopy were cryoprotected (overnight, 4°C) in 20% glycerol, phosphate-buffered saline. Brains prepared for electron microscopy were rinsed in cold phosphate-buffered saline. Coronal or sagittal sections (40 μm) were cut on a sliding microtome or Vibratome and were transferred to cold TBS (pH 7.2). Samples (~2 mm^2) were taken from Vibratome sections, treated (1 hr) with 2% osmium tetroxide, dehydrated, and flat embedded in resin [58% Araldite, 40% dodecenyl succinic anhydride, 2% 2,4,6,-tri(dimethylaminomethyl) phenol]. Plastic-embedded sections were mounted on an Araldite block and cut into semithin (1 μm) and ultrathin (gold to silver interference color) sections for light and electron microscopy, respectively. Ultrathin sections, stained with uranyl acetate and lead citrate, were viewed and photographed with a Hitachi H600 electron microscope.

Semithin slices of striatum and hippocampus (dendate gyrus) were also examined microscopically from the sides ipsilateral and contralateral to the intraventricular infusion catheter. In general, at least 4–8 semithin slices were examined from each hemisphere from each animal treated. To quantitate neurotoxicity, all neurons that exhibited abnormal cytoarchitectural, e.g., cytoplasmic vacuoles, necrosis (swelling, nuclear pyknosis) were counted in 10 random high power fields (1000×). Treatments included ACSF controls (n = 4), sense controls (n = 3–5 for each transporter subtype); and antisense oligonucleotide (n = 6–12 for each transporter subtype).

Messenger RNA

^{32}P-labeled antisense GLT-1, GLAST, and EAAC1 cRNA were generated using the Maxiscript kit (Ambion, TX). The RNA from striatal brain regions from antisense oligonucleotide and from untreated control rats was purified by RNAexpress (USB), and quantitated in ribonuclease protection assays with the riboprobes according to the manufacturer's instructions (RPA II kit, Ambion). Messenger RNA integrity was determined by hybridization of the same striatal RNA to a ^{32}P-labeled antisense rat β-actin cRNA probe (Ambion).

Glutamate Transport

Glutamate transporter sites in striatum or hippocampus were quantified by [^{3}H]-D-aspartate binding to freshly prepared P1 fraction membranes. Tissue was homogenized in 50 mM Tris–HCl (pH 7.4) and centrifuged at 1000 g for 10 min. The pellet was resuspended in Tris–HCl buffer containing 300 mM NaCl, for a protein concentration of 2 mg/ml. [^{3}H]-D-aspartate binding was measured by the addition of 50 nM [^{3}H]-D-aspartate (25 Ci/mmol, New England Nuclear, Boston, MA) to 100 μg P1 fraction membranes in a volume of 200 μl. The mixture was incubated for 20 min at 22°C, followed by rapid filtration (Cambridge Technology, Watertown, MA) over prewetted (Tris–HCl, pH 7.4, 4°C) glass fiber filters (Cambridge Technology). Nonspecific binding was determined by [^{3}H]-D-aspartate binding in the presence of 100 μm DL-threo-β-hydroxyaspartate.

Microdialysis

Male Sprague–Dawley rats weighing 250–300 g were implanted intraventricularly with stainless steel cannulas (Alzet brain infusion kit, ALZA Corp., CA; stereo coordinates: −1.0 mm anterior–posterior; −1.4 mm lateral; approximately −4.0 mm dorsoventral) using a pressure transducer to assure placement in the ventricle. ACSF with either sense or antisense (2.5 mg/ml CSF solution) was continuously delivered through an Alzet mini-osmotic pump (#2002, ALZA Corp.) at 1 μl/hr into the right lateral cerebral ventricle for 7 days. After 7 days of oligonucleotide treatment, a microdialysis probe (CMA/12, 2 mm) was placed in the ipsilateral striatum (stereo coordinates: −1 mm anterior–posterior; −3.0 mm lateral; approximately −3.8 mm dorsoventral). Dialyzates were collected automatically into 200 μl glass minivials, maintained at 4°C, at 30 min intervals, using a flow rate of 2 μl/min. Amino acid analysis of dialyzates (20 μl) was performed by reverse phase high pressure liquid chromatography using precolumn derivatization and fluorescence detection for glutamate and asparagine (Shimada et al., 1993). In vitro probe recovery was determined after the in vivo experiment by placing the probe in a plastic vial (2 ml) containing a known concentration of amino acids. The brain extracellular fluid concentration was calculated by dividing the in vivo dialyzate concentration by the in vitro recovery.

Statistical Analysis

Analysis of changes in treatment groups was performed using Student's t test.

Acknowledgements

We thank Dr. David Borchelt for his scientific advice and helpful discussions during the course of this work. This study was funded in part from grants from the National Institutes of Health–National Institute of Neurological Disorders and Stroke (NS33958; AG12992), the Muscular Dystrophy Association, and the Jay Slotkin Fund for Neuromuscular Research.

The costs of publication of this article were defrayed in part by the payment of page charges. This article must therefore be hereby marked *"advertisement"* in accordance with 18 USC Section 1734 solely to indicate this fact.

Received October 3, 1995; revised December 13, 1995.

References

Arriza, J.L., Fairman, W.A., Wadiche, J.I., Murdoch, G.H., Kavanaugh, M.P., and Amara, S.G. (1994). Functional comparisons of three glutamate transporter subtypes cloned from human motor cortex. J. Neurosci. *14*, 5559–5569.

Attwell, D., Barbour, B., and Szatkowski, M. (1993). Nonvesicular release of neurotransmitter. Neuron *11*, 401–407.

Barks, J.D.E., and Silverstein, F.S. (1994). The glutamate uptake inhibitor L-*trans*-2,4-pyrrolidine dicarboxylate is neurotoxic in neonatal rat brain. Mol. Chem. Neuropath. *23*, 201–211.

Fairman, W.A., Vandenberg, R.J., Arriza, J.L., Kavanaugh, M.P., and Amara, S.G. (1995). An excitatory amino-acid transporter with properties of a ligand-gated chloride channel. Nature *375*, 599–603.

Hajos, F., Garthwaite, G., and Garthwaite, J. (1986). Reversible and irreversible neuronal damage caused by excitatory amino acid analogues in rat cerebellar slices. J. Neurosci. *18*, 417–436.

Hertz, L. (1979). Functional interactions between neurons and astrocytes. I. Turnover and metabolism of putative amino acid transmitters. Prog. Neurobiol. *13*, 277–323.

Isaacson, J.S., and Nicoll, R.A. (1993). The uptake inhibitor L-*trans*-PDC enhances responses to glutamate but fails to alter the kinetics of excitatory synaptic currents in the hippocampus. J. Neurophysiol. *70*, 2187–2191.

Kanai, Y., and Hediger, M. (1992). Primary structure and functional characterization of a high affinity glutamate transporter. Nature *360*, 467–471.

Kanai, Y., and Hediger, M.A. (1995). High affinity glutamate transporters: physiological and pathophysiological relevance in the central nervous system. In Excitatory Amino Acids, D.W. Brann and V.B. Mahesh, eds. (Boca Ratan, FL: CRC Press), in press.

Kanai, Y., Bhide, P.G., Difiglia, M., and Hediger, M.A. (1995a). Neuronal high affinity glutamate transport in the rat central nervous system. Neuroreport, *6*, 2357–2362.

Kanai, Y., Nussberger, S., Romero, M.F., Boron, W.F., Hebert, S.C., and Hediger, M.A. (1995b). Electrogenic properties of the epithelial and neuronal high affinity glutamate transporter. (1995). J. Biol. Chem. *270*, 16561–16568.

Lehre, K.P., Levy, L.M., Ottersen, O.P., Storm-Mathisen, J., and

Danbolt, N.C. (1995). Differential expression of two glutamate transporters in rat brain: quantitative and immunocytochemical observations. J. Neurosci. *15*, 1835–1853.

Maki, R., Robinson, M.B., and Dicter, M.A. (1994). The glutamate uptake inhibitor L-*trans*- pyrrolidine-2,4-dicarboxylate depresses excitatory synaptic transmission via a presynaptic mechanism in cultured hippocampal neurons. J. Neurosci. *14*, 6754–6762.

Mennerick, S., and Zorumski, C.F. (1994). Glial contributions to excitatory neurotransmission in cultured hippocampal cells. Nature *368*, 59–62.

Merlis, J.K. (1940). Artificial cerebrospinal fluid. Amer. J. Physiol. *131*, 67–72.

Nicholls, D., and Attwell, D. (1990). The release and uptake of excitatory amino acids. Trends Pharmacol. Sci. *11*, 462–468.

Norenberg, M.D., and Martinez-Hernandez, A. (1979). Fine structural localization of glutamine synthetase in astrocytes in brain. Brain Res. *161*, 303–310.

Olney, J.W. (1969). Glutamate-induced retinal degeneration in neonatal mice. Electron microscopy of the acutely evolving lesion. J. Neuropath. Exp. Neurol. *28*, 455–474.

Olney, J.W., DeGubareff, T., and Sloviter, R.S. (1983). "Epileptic" brain damage in rats induced by sustained electrical stimulation of the perforant path. II. Ultrastructural analysis of acute hippocampal pathology. Brain Res. Bull. *10*, 699–712.

Pines, G., Danbolt, N.C., Bjoras, M., Zhang, Y., Bendahan, A., Eide, L., Koepsell, H., Storm-Mathisen, J., Seeberg, E., and Kanner, B.I. (1992). Cloning and expression of a rat brain L-glutamate transporter. Nature *360*, 464–467.

Pow, D.V., and Robinson, S.R. (1994). Glutamate in some retinal neurons is derived soley from glia. Neuroscience *60*, 355–366.

Riepe, R.E., and Norenberg, M.D. (1977). Müeller cell localisation of glutamine synthetase in rat retina. Nature *268*, 654–656.

Robinson, M.B., Djali, S., and Buchhalter, J.R. (1993). Inhibition of glutamate uptake with L-*trans*-pyrrolidine-2,4-dicarboxylate potentiates glutamate toxicity in primary hippocampal cultures. J. Neurochem. *61*, 2099–2103.

Rothstein, J.D., and Kuncl, R.W. (1995). Neuroprotective strategies in a model of chronic glutamate-mediated motor neuron toxicity. J. Neurochem. *65*, 643–651.

Rothstein, J.D., Martin, L.J., and Kuncl, R.W. (1992). Decreased brain and spinal cord glutamate transport in amyotrophic lateral sclerosis. New Engl. J. Med. *326*, 1464–1468.

Rothstein, J.D., Jin, L., Dykes-Hoberg, M., and Kuncl, R.W. (1993). Chronic glutamate uptake inhibition produces a model of slow neurotoxicity. Proc. Natl. Acad. Sci. USA *90*, 6591–6595.

Rothstein, J.D., Martin, L., Levey, A.I., Dykes-Hoberg, M., Jin, L., Wu, D., Nash, N., and Kuncl, R.W. (1994). Localization of neuronal and glial glutamate transporters. Neuron *13*, 713–725.

Rothstein, J.D., Van Kammen, M., Levey, A.I., Martin, L., and Kuncl, R.W. (1995). Selective loss of glial glutamate transporter GLT-1 in amyotrophic lateral sclerosis. Ann. Neurol. *38*, 73–84.

Sarantis, M., Ballerini, L., Miller, B., Silver, R.A., Edwards, M., and Attwell, D. (1993). Glutamate uptake from the synaptic cleft does not shape the decay of non-NMDA component of the synaptic current. Neuron *11*, 541–549.

Shaw, P.J., Chinnery, R.M., and Ince, P.G. (1994). [^{3}H]D-aspartate binding sites in the normal human spinal cord and changes in motor neuron disease: a quantitative autoradiographic study. Brain Res. *655*, 195–201.

Shimada, N., Graf, R., Rosner, G., and Heiss, W.D. (1993). Ischemia-induced accumulation of extracellular amino acids in cerebral cortex, white matter, and cerebrospinal fluid. J. Neurochem. *60*, 66–71.

Storck, T., Schulte, S., Hofmann, K., and Stoffel, W. (1992). Structure, expression, and functional analysis of a Na^+-dependent glutamate/aspartate transporter from rat brain. Proc. Natl. Acad. Sci. USA *89*, 10955–10959.

Tong, G., and Jahr, C.E. (1994). Block of glutamate transporters potentiates postsynaptic excitation. Neuron *13*, 1195–1203.

Wagner, R.W. (1994). Gene inhibition using antisense oligodeoxynucleotides. Nature *372*, 333–335.

Whitesell, L., Geselowitz, D., Chavany, C., Fahmy, B., Walbridge, S., Alger, J.R., and Neckers, L.M. (1993). Stability, clearance, and disposition of intraventricularly administered oligodeoxynucleotides: implications for therapeutic application within the central nervous system. Proc. Natl. Acad. Sci. USA *90*, 4665–4669.